

Available online at [www.sciencedirect.com](http://www.sciencedirect.com)

ScienceDirect

journal homepage: [www.elsevier.com/locate/radcr](http://www.elsevier.com/locate/radcr)

## Case Report

# A large benign struma ovarii with atypical imaging findings <sup>☆</sup>

Kaiji Inoue<sup>a,\*</sup>, Eri Hoshino<sup>a</sup>, Taira Shiratori<sup>a</sup>, Atsushi Sasaki<sup>b</sup>, Takeshi Kajihara<sup>c</sup>, Eito Kozawa<sup>a</sup>

<sup>a</sup>Department of Radiology, Saitama Medical University Hospital, Saitama, Japan

<sup>b</sup>Department of Pathology, Saitama Medical University International Medical Center, Saitama, Japan

<sup>c</sup>Department of Obstetrics and gynecology, Saitama Medical University Hospital, Saitama, Japan

## ARTICLE INFO

## Article history:

Received 10 June 2024

Revised 9 August 2024

Accepted 10 August 2024

## Keywords:

Ovarian tumor

Struma ovarii

Solid component

Magnetic resonance imaging

Atypical imaging findings

## ABSTRACT

Struma ovarii is a mature ovarian teratoma characterized by the predominant presence of thyroid-tissue components. Typically, struma ovarii presents as relatively small masses (<10 cm) that often appear as multilocular cystic tumors with solid components. Herein, we report the unique case of a 44-year-old female with a large tumor including a solid mass. The solid components of the tumor comprised typical thyroid tissues with multiple small cystic structures containing colloid-like material. Given the rarity of struma ovarii, atypical imaging features can sometimes be misleading. This article highlights the unusual magnetic resonance imaging characteristics of a large struma ovarii, with a specific focus on the presence of solid components.

© 2024 The Authors. Published by Elsevier Inc. on behalf of University of Washington.

This is an open access article under the CC BY-NC-ND license

(<http://creativecommons.org/licenses/by-nc-nd/4.0/>)

## Introduction

Struma ovarii is a mature ovarian teratoma primarily composed of thyroid-tissue components and is an exceedingly rare tumor [1,2]. Struma ovarii typically presents as relatively small masses (<10 cm), that often appear as multilocular cystic tumors with solid components [1,3]. Herein, we report an unusual case involving a large struma ovarii with significant solid components. Emphasizing the presence of large solid components, this article provides a comprehensive review of the literature on this rare type of ovarian tumor.

## Case report

A 44-year-old, gravida 0, para 0 woman presented to our hospital complaining of sudden lower abdominal pain while walking. The patient had been treated for infertility for 10 years, and no significant findings were detected on routine ultrasonography at that time. During the internal examination, a neonatal-sized soft mass was palpated on the anterior surface of the uterus, without any tenderness. Laboratory tests revealed a slightly elevated serum cancer antigen 125 level (56.3 ng/mL; normal level < 35 ng/mL). Other tumor markers,

<sup>☆</sup> Competing Interests: The authors declare that they have no known competing financial interests or personal relationships that could have appeared to influence the work reported in this paper.

\* Corresponding author.

E-mail address: [kaiji@saitama-med.ac.jp](mailto:kaiji@saitama-med.ac.jp) (K. Inoue).

<https://doi.org/10.1016/j.radcr.2024.08.048>

1930-0433/© 2024 The Authors. Published by Elsevier Inc. on behalf of University of Washington. This is an open access article under the CC BY-NC-ND license (<http://creativecommons.org/licenses/by-nc-nd/4.0/>)

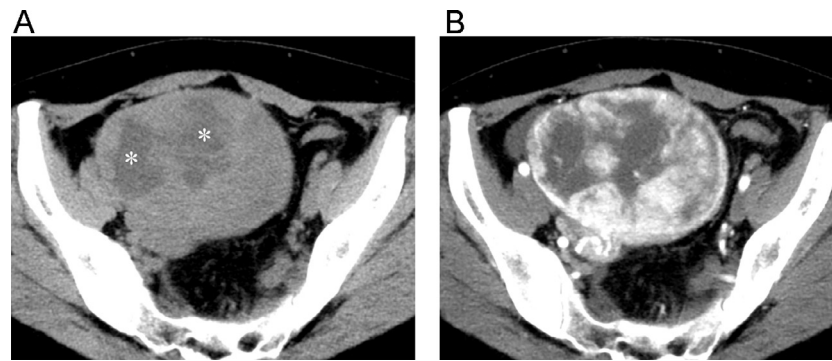


**Fig. 1 – CT images showing an ovoid-shaped solid mass measuring  $12 \times 9 \times 8 \text{ cm}^3$  arising from the right ovary. (A) Nonenhanced CT shows a mass with central areas with low density (indicated with asterisks) and peripheral areas with iso density compared to muscles. (B) In the early phase, contrast-enhanced CT shows heterogeneous enhancement of the peripheral areas of the mass. CT: computed tomography.**

including cancer antigen 19–9 (11.7 U/mL; normal level  $\leq 37$  U/mL), carcinoembryonic antigen (1.0 ng/mL; normal level  $< 5.0$  ng/mL), human chorionic gonadotropin (2.1 mIU/mL; normal level  $\leq 3.0$  mIU/mL),  $\alpha$ -fetoprotein (2.1 ng/mL; normal level  $\leq 10.0$  ng/mL), and human epididymis protein 4 (47.3 pmol/L; normal level  $\leq 70.0$  pmol/L) were all within normal ranges. Since there were no symptoms of hyperthyroidism, such as palpitations, hyperhidrosis, or tremor of the limbs, thyroid function tests were not performed.

Abdominal ultrasound revealed a  $10 \times 8 \text{ cm}^2$  mass in the pelvis with uneven blood flow. Computed tomography (CT) was performed to rule out any emergency gynecological diseases and revealed a smooth ovoid solid mass with cystic components measuring  $12 \times 9 \times 8 \text{ cm}^3$  in the right adnexal region (Fig. 1). On nonenhanced CT (Fig. 1A), the mass demonstrated heterogeneous low density, with no calcification or fatty component. Contrast-enhanced CT revealed a solid component with strong contrast enhancement and several cystic areas with low attenuation and no contrast enhancement in the early phase (Fig. 1B).

Magnetic resonance imaging (MRI) was performed to evaluate the ovoid mass in the right ovary (Fig. 2). On T2-weighted images, the mass consisted of a low-intensity solid component and numerous high-intensity cystic components (Fig. 2A). On fat-suppressed T1-weighted images, the solid components showed a signal intensity comparable to that of skeletal muscle, whereas the cystic components showed low intensity (Fig. 2B). Dynamic contrast revealed strong partial enhancement of the solid components in the early phase (Fig. 2C), followed by the spread of the contrast effect over all solid components in the delayed phase (Fig. 2D).

Our preoperative radiological diagnosis was sclerosing stromal tumor of the ovary, mainly based on the presence of a solid and hypervascular tumor in a menopausal woman. The differential diagnosis was a malignant epithelial stromal tumor.

The patient underwent right salpingo-oophorectomy. Macroscopically, the tumor appeared as an ovoid solid mass with cystic components (Fig. 3A). Microscopically,

thyroid-tissue follicles of various sizes were observed using hematoxylin and eosin staining (Fig. 3B:  $\times 40$ , 3C:  $\times 200$ ). The pathological diagnosis was struma ovarii of the right ovary. The patient showed no signs of local or distal recurrence for 2 years postoperatively.

## Discussion

Struma ovarii is a rare specialized mature ovarian teratoma that accounts for nearly 3% of ovarian teratomas [1,2] and is characterized by thyroid-tissue components constituting  $>50\%$  of the overall tissue [1,2]. Most cases are asymptomatic and incidentally found during imaging examinations for other purposes. Struma ovarii typically occurs in women aged 20–40 years, similar to mature cystic teratoma, and the incidence of struma ovarii peaks in the fifth decade of life [1,2]. The symptoms are usually nonspecific and similar to those of mature cystic teratomas. Hyperthyroidism occurs in 5%–8% of patients [4]. Benign struma ovarii typically have a good prognosis, and treatment necessitates surgical removal of the ovary, which is usually sufficient. Malignant struma ovarii are less common, with no standardized treatment or well-evaluated prognosis. Given the similarities with thyroid cancer, the general consensus is to treat malignant struma ovarii like thyroid cancer—with surgical tumor resection and adjuvant radioactive iodine therapy [5]. Accurate preoperative radiological imaging diagnosis of struma ovarii is important to avoid unnecessary surgery because 95% of struma ovarii are benign and occur in premenopausal women, although the MRI findings are similar to those of malignant ovarian tumors [6].

MRI is a valuable diagnostic tool for assessing ovarian lesions, including malignant and benign tumors. Several studies have reported the MRI characteristics of struma ovarii, which include a unilateral multilocular mass with solid components and thick septations that shows low signal intensity on T2-weighted images [7–10,12]. Heightened contrast enhancement

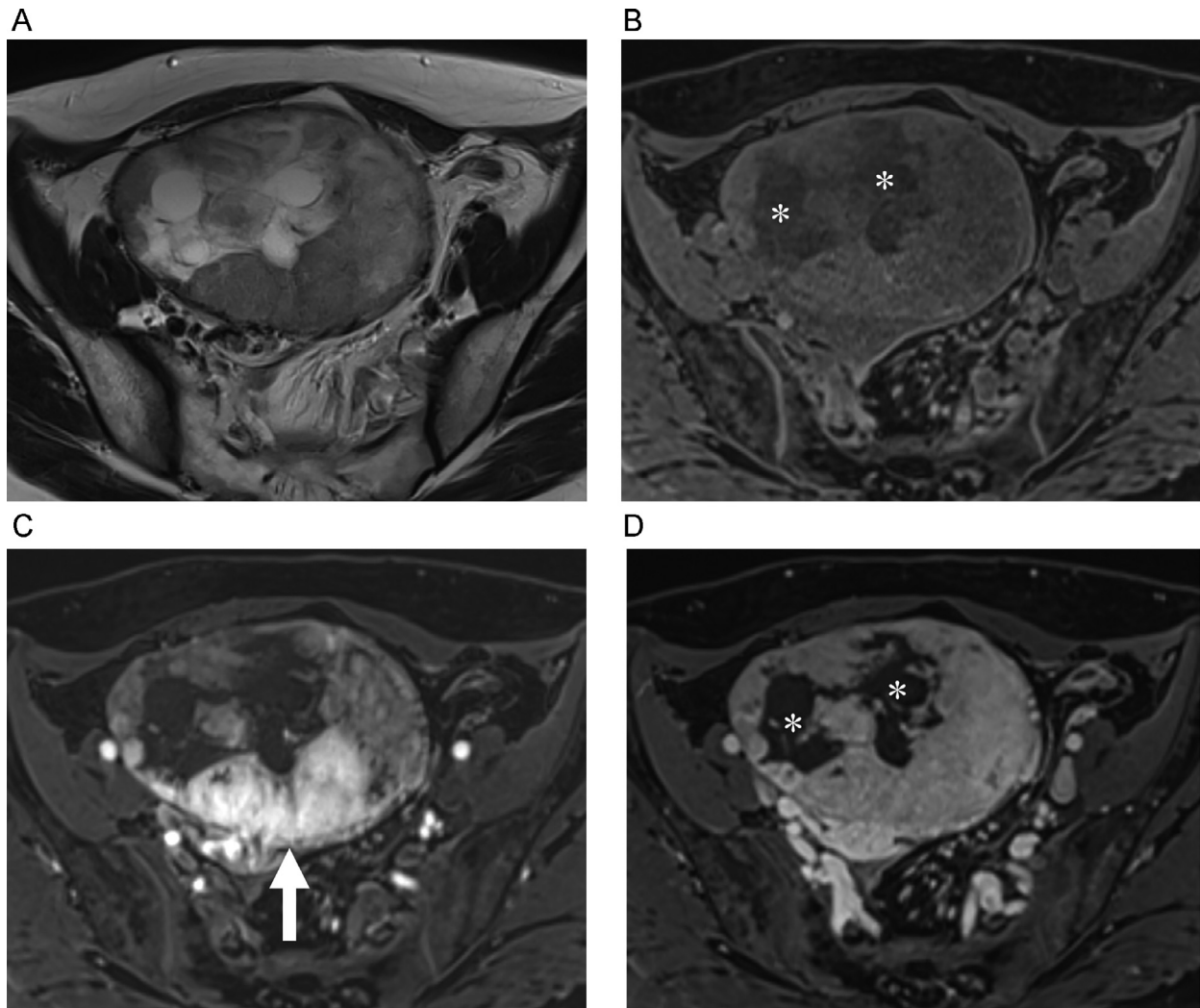


**Fig. 2 – MRI shows an ovoid-shaped mass in the right ovary. (A) On axial T2-weighted image, the mass appears heterogeneous with high signal intensity. (B) Fat-saturated axial T1-weighted image shows that the central zone has low intensity (indicated with asterisks) and peripheral areas are almost iso intense compared to muscles. (C) In the early phase of enhanced fat-saturated axial T1-weighted imaging, part of the peripheral area (indicated with an arrow) of the tumor shows a strong contrast enhancement. (D) In the late phase of enhanced fat-saturated axial T1-weighted imaging, cystic components (indicated with asterisks) are observed in part of central area of the tumor. Additionally, moderately enhancing solid components are seen.**

**MRI: magnetic resonance imaging.**

is attributed to the presence of thyroid tissue, which thickens the septa or nodules [11–13]. The characteristic features on CT include high attenuation on noncontrast CT images. This phenomenon is attributed to the thyroid follicles containing gelatinous colloid materials rich in thyroid hormones and iodine compounds [14]. In the present case, the cystic components exhibited low density on noncontrast CT and high signal intensity on T2-weighted magnetic resonance images. However, signal intensity of struma ovarii varies based on the proportion of gelatinous colloid material containing thyroid hormones, and T2-weighted images may manifest a stained-glass pattern [9,14]. The presence of hemorrhage, necrosis, or fibrosis within the cystic components may further influence the signal intensity of the cysts.

Dujardin et al. reported that multiple small cystic components in markedly or moderately enhancing solid components on MRI were characteristic of struma ovarii [12]. They reported that multiple small cystic components with thick septa and small nodules in the markedly or moderately enhancing solid components resulted in a "lacy appearance" [12]. However, we could not detect this imaging feature because our patient presented with large solid components on MRI. Histopathologically, in the area initially thought to be the solid component, a dense cystic structure with thick septa and small nodules consisting of very small thyroid follicles was identified. Therefore, small cystic structures that result in the characteristic lace-like pattern of struma ovarii may not have been readily identified on contrast-enhanced T1-weighted MRI. In the present



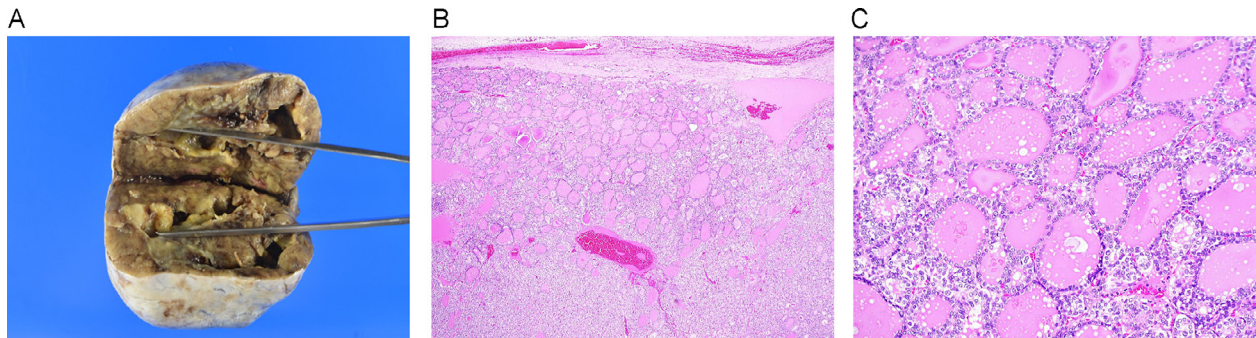


**Fig. 3 – Pathological findings. (A) Macroscopically, the tumor appears as an ovoid solid mass with cystic components. (B) Microscopic examination reveals thyroid tissue within follicles of variable size and no necrotic or mitotic areas (H&E staining,  $\times 40$ ). (C) The high-magnification view shows thyroid follicles of various sizes lined by cuboidal epithelial cells and filled with colloid (H&E staining,  $\times 200$ ).**

**H&E: hematoxylin and eosin.**

case, a sclerosing stromal tumor was considered the primary differential diagnosis based on the pronounced contrast effect caused by the congestion of numerous small cystic structures, including solid components. Notably, in our study, the tumor did not exhibit high attenuation on noncontrast CT. This deviation may also be attributed to the relatively small size of the cystic components.

## Conclusions

We reported a rare case of struma ovarii comprising a large tumor with significant solid components. Imaging findings of struma ovarii may be atypical depending on the cyst size and concentration of the contents. Future reports of cases will help determine the cause.

## Author contributions

All authors provided final approval of the submitted version.

## Data availability

Our submission is a case report. Therefore, the data used to support the findings of this case report are included in this article. No additional data are available because this is a case report.

## Patient consent

Written informed consent for the publication of this case report was obtained from the patient.

## REFERENCES

- [1] Maniar KP, Vang V. Germ cell tumors of the ovary. In: Kurman RJ, Ellenson LH, Ronnett BM, editors. *Blaustein's Pathology of the Female Genital Tract*. Cham, Switzerland: Springer; 2019. p. 1087–9. ISBN 978-3-319-46333-9. doi:10.1007/978-3-319-46334-6.
- [2] Shaco-Levy R, Fukunaga M, Stewart CJR. Struma ovarii. In: Köbel M, Huntsman DG, Lim D, editors. *WHO Classification of Tumours*. Lyon: IARC Press; 2020. p. 132–3. ISBN 9789283245049.
- [3] Park SB, Kim JK, Kim K, Cho K. Imaging findings of complications and unusual manifestations of ovarian teratomas. *Radiographics* 2008;28:969–83. doi:10.1148/rg.284075069.
- [4] Makani S, Kim W, Gaba AR. Struma ovarii with a focus of papillary thyroid cancer: a case report and review of the literature. *Gynecol Oncol* 2004;94:835–9. doi:10.1016/j.ygyno.2004.06.003.
- [5] Rockson O, Kora C, Ramdani A, Basma A, Bouhout T, Serji B, et al. Struma ovarii: two case reports of a rare teratoma of the ovary. *J Surg Case Rep* 2020;2020:rjaa493. doi:10.1093/jscr/rjaa493.
- [6] Alvarez DM, Lee V, Bhatt S, Dogra VS. Struma ovarii with papillary thyroid carcinoma. *J Clin Imaging Sci* 2011;1:44. doi:10.4103/2156-7514.84322.
- [7] Matsuki M, Kaji Y, Matsuo M, Kobashi Y. Struma ovarii: MRI findings. *Br J Radiol* 2000;73:87–90. doi:10.1259/bjr.73.865.10721328.
- [8] Kim JC, Kim SS, Park JY. MR findings of struma ovarii. *Clin Imaging* 2000;24:28–33. doi:10.1016/s0899-7071(00)00158-3.
- [9] Joja I, Asakawa T, Mitsumori A, Nakagawa T, Hiraki Y, Kudo T, et al. Struma ovarii: appearance on MR images. *Abdom Imaging* 1998;23:652–6. doi:10.1007/s002619900424.
- [10] Yamashita Y, Hatanaka Y, Takahashi M, Miyazaki K, Okamura H. Struma ovarii: MR appearances. *Abdom Imaging* 1997;22:100–2. doi:10.1007/s002619900150.
- [11] Fujiwara S, Tsuyoshi H, Nishimura T, Takahashi N, Yoshida Y. Precise preoperative diagnosis of struma ovarii with pseudo-Meigs' syndrome mimicking ovarian cancer with the combination of  $^{131}\text{I}$  scintigraphy and  $^{18}\text{F}$ -FDG PET: case report and review of the literature. *J Ovarian Res* 2018;11:11. doi:10.1186/s13048-018-0383-2.

- 
- [12] Dujardin MI, Sekhri P, Turnbull LW. Struma ovarii: role of imaging? *Insights Imaging* 2014;5:41–51. doi:[10.1007/s13244-013-0303-3](https://doi.org/10.1007/s13244-013-0303-3).
- [13] Shen J, Xia X, Lin Y, Zhu W, Yuan J. Diagnosis of struma ovarii with medical imaging. *Abdom Imaging* 2011;36:627–31. doi:[10.1007/s00261-010-9664-y](https://doi.org/10.1007/s00261-010-9664-y).
- [14] Ikeuchi T, Koyama T, Tamai K, Fujimoto K, Mikami Y, Konishi I, et al. CT and MR features of struma ovarii. *Abdom Imaging* 2012;37:904–10. doi:[10.1007/s00261-011-9817-7](https://doi.org/10.1007/s00261-011-9817-7).